



Stress concentration factors for planar square cell lattices with filleted junctions

Michele Dallago | Sunil Raghavendra | Vigilio Fontanari | Matteo Benedetti

Dipartimento di Ingegneria Industriale,
Università degli Studi di Trento, Via
Sommarive, Trento, Italy

Correspondence

M. Dallago, Università degli Studi di
Trento - Dipartimento di Ingegneria
Industriale - Via Sommarive, 9, 38123
Trento, Italy.
Email: michele.dallago@unitn.it

Abstract

The estimation of the fatigue resistance of cellular structures is fundamental in many applications. The maximum stresses in a material determine the fatigue resistance of the component. In this work, a numerical method is proposed for the estimation of the Stress Concentration Factors (SCF) at the cell wall junctions of 2D cellular structures based on square unit cells. The aim is to obtain a model capable of calculating the values of the SCF as a function of the unit cell geometrical parameters, namely the cell-wall thickness t_0 and the fillet radius R at the joints. This was achieved by applying the Finite Elements (FE) method to the unit cell for wide intervals of t_0 and R to calculate the SCF for each couple of the parameters. The values of the SCFs were then fitted with some functions.

KEYWORDS

cellular structures, finite elements, stress concentration factor

1 | INTRODUCTION

The advent of Additive Manufacturing gave a considerable boost to the study of cellular materials because the new 3D printing processes, such as Selective Laser Melting (SLM), permit to obtain products with dimensional accuracy less than 0.2 millimeters, giving the possibility of fabricating, in minute details, components made of complex lattice structures. These premises highlight the importance of studying filleted joints in cellular materials as they can be introduced into the design phase to reduce stress concentrations.¹ Indeed, tensile fatigue tests show that fatigue cracks in SLM lattices occur at the joints,² indicating that the shape of the joints is critical in determining the fatigue behavior of this type of structures.³ In fact, the positive effect of filleted joints on the fatigue resistance of cellular structures was shown by Abad et al.¹ On the other hand, fillets at junctions can be unwanted, but generated due to the accumulation of parasitic mass at the strut joints in some AM processes such as SLM.⁴

In this work, a numerical method is proposed to estimate the SCFs at the cell wall junctions of 2D regular square cell cellular structures. This type of lattice can be viewed as an infinite plate with a regular distribution of square holes with rounded edges. In the literature there are several studies concerning the stress distribution around holes of various geometries in infinite plates. Nevertheless, to the best of our knowledge, there are no solutions available to compute the stress distribution in plates with a regular distribution of square holes with rounded corners. Indeed, the closed form solutions provided refer to a single hole,^{5,6} double holes⁷ or, at most, an infinite array⁸ in an infinite plate. Such cases, despite being close to the problem examined in our work, clearly do not capture accurately the stress distribution at the filleted junctions of the cellular lattice. Moreover, due to the complexity of the analytical approaches (generally based on the complex-variable method), the analytical solutions are often limited to the uniaxial tension case. Therefore, the aim is to obtain a model capable of calculating the values of the SCFs as a function of the unit cell geometrical parameters,

namely the cell-wall thickness t_0 and the fillet radius R at the joints, for any in-plane load case. This was achieved by applying the FE method to the unit cell for wide intervals of t_0 and R normalized by the unit cell size L , $t_0^* = \frac{t_0}{L}$ and $R^* = \frac{R}{L}$, to calculate the SCF for each couple of the parameters. The values of the SCF were then fitted with some functions. This work is an effort to provide a useful semi-analytical instrument that allows the designer to estimate the maximum stress in a structure by avoiding lengthily numerical simulations. This model has similar basis to that of Dallago et al.,⁹ which is aimed at predicting the elastic constants of the same type of lattices. Indeed, the present model can be coupled with the model for the elastic constants to identify the geometrical parameters of a 2D lattice that minimize the stress concentrations while controlling the values assumed by the elastic constants. This can be very useful in the design of load bearing biomedical lattices, where the value of the elastic modulus is of paramount importance to improve biocompatibility.¹⁰ Moreover, our model can be the starting base also for the study of 3D lattices.

1.1 | Model development

The effect of the filleted cell-wall junctions of square cell lattices (Figure 1a) on the local stress field is represented by the equivalent stress concentration factor K_{eq} . This factor is defined in Equation (1) as the ratio between the maximum equivalent stress $\bar{\sigma}$ at the fillet (as indicated in Figure 1c) and the equivalent stress calculated from the nominal stress components acting on the unit cell $\bar{\sigma}_n$ (as indicated in Figure 1b). The equivalent stresses are calculated from the stress components according to the von Mises criterion because it is one of the most used for ductile metals,¹¹ but in principle any other criterion could be used. Regarding fatigue design, using the geometrical stress concentration factor instead of the fatigue notch factor is conservative as it intrinsically assumes a notch sensitivity of 1 and, moreover, it decouples this analysis from the material properties.

$$K_{eq} = \frac{\bar{\sigma}}{\bar{\sigma}_n} \quad (1)$$

The definition of Equation (1) is based on the observation that lattice structures can be considered continuous homogenous materials if the unit cell is infinitesimally small if compared to the size of the lattice. Consequently, the stress tensor in a point of the lattice material can be applied to the unit cell as the nominal stresses shown in Figure 1b. In real applications, the unit cell has finite dimensions and the larger the unit cell compared to the macroscopic part, the less accurate becomes this procedure.

The maximum local stress components on the fillet are related to the nominal stress components by a stress concentration factors matrix \mathbf{K} (Equation (2)).

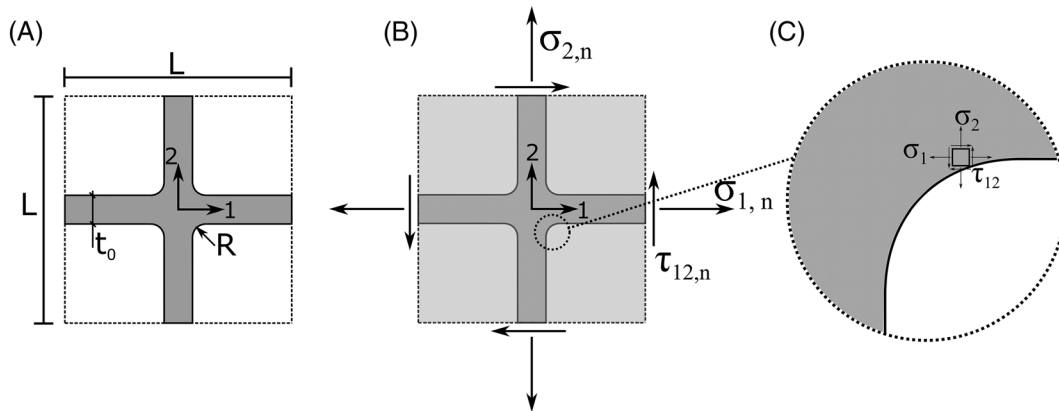


FIGURE 1 Regular 2D square unit cell cellular material with filleted junctions: (a) unit cell geometry; (b) nominal plane stress components acting on the unit cell sides; (c) infinitesimal square element in the 1–2 reference system defining the local stresses at the fillet. The 1–2 cartesian reference system indicates the material principal directions.

$$\begin{Bmatrix} \sigma_1 \\ \sigma_2 \\ \tau_{12} \end{Bmatrix} = \mathbf{K} \begin{Bmatrix} \sigma_{1,n} \\ \sigma_{2,n} \\ \tau_{12,n} \end{Bmatrix} = \begin{bmatrix} K_{1,1} & K_{1,2} & K_{1,12} \\ K_{2,1} & K_{2,2} & K_{2,12} \\ K_{12,1} & K_{12,2} & K_{12,12} \end{bmatrix} \begin{Bmatrix} \sigma_{1,n} \\ \sigma_{2,n} \\ \tau_{12,n} \end{Bmatrix} \quad (2)$$

If the nominal stress components are divided by the nominal equivalent stress $\bar{\sigma}_n$, and thus the $R_1 = \frac{\sigma_{1,n}}{\bar{\sigma}_n}$, $R_2 = \frac{\sigma_{2,n}}{\bar{\sigma}_n}$ and $R_{12} = \frac{\tau_{12,n}}{\bar{\sigma}_n}$ ratios are defined, Equation (2) can be rewritten explicitly as a function of these non-dimensional ratios:

$$\sigma_1 = (K_{1,1}R_1 + K_{1,2}R_2 + K_{1,12}R_{12})\bar{\sigma}_n = C_1\bar{\sigma}_n \quad (3a)$$

$$\sigma_2 = (K_{2,1}R_1 + K_{2,2}R_2 + K_{2,12}R_{12})\bar{\sigma}_n = C_2\bar{\sigma}_n \quad (3b)$$

$$\tau_{12} = (K_{12,1}R_1 + K_{12,2}R_2 + K_{12,12}R_{12})\bar{\sigma}_n = C_{12}\bar{\sigma}_n \quad (3c)$$

Substituting Equations (3) into the definition of von Mises equivalent stress in plane stress and then into Equation (1) leads to the expression that relates the equivalent stress concentration factor K_{eq} to the components of the \mathbf{K} matrix and the nominal stresses on the unit cell.

$$K_{eq} = \frac{\bar{\sigma}}{\bar{\sigma}_n} = \frac{\sqrt{\bar{\sigma}_n^2 C_1^2 + \bar{\sigma}_n^2 C_2^2 - \bar{\sigma}_n^2 C_1 C_2 + 3\bar{\sigma}_n^2 C_{12}^2}}{\bar{\sigma}_n} = \sqrt{C_1^2 + C_2^2 - C_1 C_2 + 3C_{12}^2} \quad (4)$$

The components of \mathbf{K} depend exclusively on the geometrical parameters of the junction (t_0 and R) and can be easily calculated with FE simulations. If the components of \mathbf{K} are calculated for wide intervals of the geometrical parameters and are then fitted with appropriate functions of t_0 and R to be substituted into Equations (4), the desired expression for K_{eq} is obtained. Such equation will be only function of the geometry and the nominal loads on the unit cell.

1.1. Finite element model and calculation of the components of K

The nine components of the \mathbf{K} matrix were obtained by solving a parametric 2D FE model of the unit cell (Figure 2a) with the boundary conditions derived from the definition of the stress concentration factors matrix according to Equation (2) (Figure 2b, 2c, 2d). The cell wall thickness-to-length ratio t_0/L of the parametric FE model was varied in the [0.02–0.2] interval, while the fillet radius-to-cell wall length ratio R/L was varied in the [0.01–0.15] interval, both with a step of 0.01. The FE model of the unit cells was built in ANSYS® and meshed with 2D 8-node structural elements with quadratic displacement behavior (PLANE183) and plane stress formulation. A convergence analysis was carried out on the mesh and it was deemed acceptable when the deviation of the von Mises equivalent stress with respect to the finest mesh was below 0.5%.

Despite the procedure illustrated above seems quite straightforward, there is a considerable issue: the location of the point on the fillet where the local stresses σ_1 , σ_2 , τ_{12} should be extracted. Considering Equation (1), all the components of the \mathbf{K} matrix should be calculated in the point in which the highest equivalent local stress is reached. This unfortunately is not trivial because the position of this point, besides the geometry, depends on the ratio between the nominal stress components acting on the unit cell, which is not known a-priori. This issue is solved by extracting the values of the stresses from the FE model along the fillet radius as a function of an angle α (Figure 3) and then calculating the components of \mathbf{K} for each α . From these data, it was possible to establish that, for each geometry, the maximum equivalent stress occurs in a point close to A (prevalently monoaxial load along direction 1) or C (prevalently monoaxial load along direction 2) or both, in the case of pure shear or biaxial loading in wide fillet radii. On the other hand, point B is critical in the case of pure shear or biaxial loading for sharp fillets. It is thus clearly impossible to find a single point on the fillet to use as a reference to calculate \mathbf{K} before having calculated K_{eq} . Therefore, the only viable strategy is to calculate the components of \mathbf{K} at each of the three points and then retain only those that correspond to the location of the highest K_{eq} . For practical reasons, locations A, B and C are kept the same

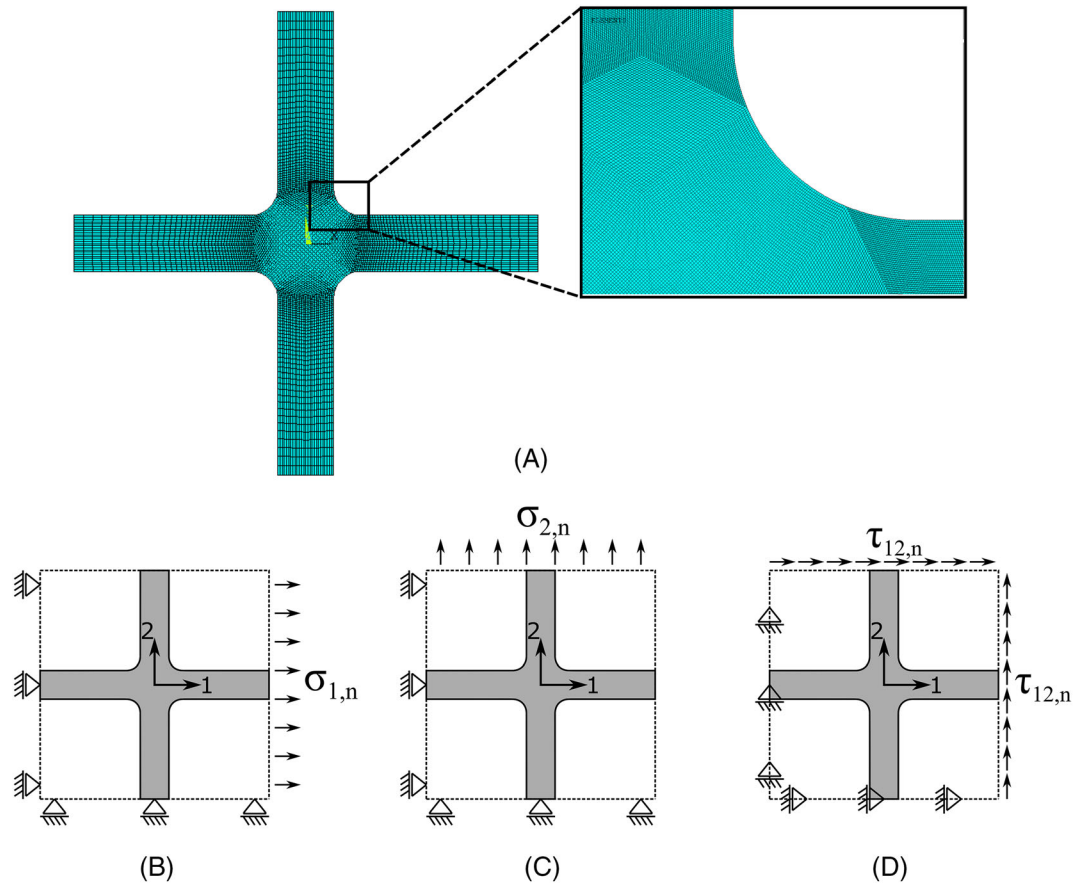


FIGURE 2 (a) Parametric FE model used to calculate the components of the SCF matrix and boundary conditions to calculate the components of the SCFs matrix: (b) pure traction along direction 1 to calculate the first column of K ; (c) pure traction along direction 2 to calculate the second column of K ; (d) pure shear in the 1–2 plane to calculate the third column of K .

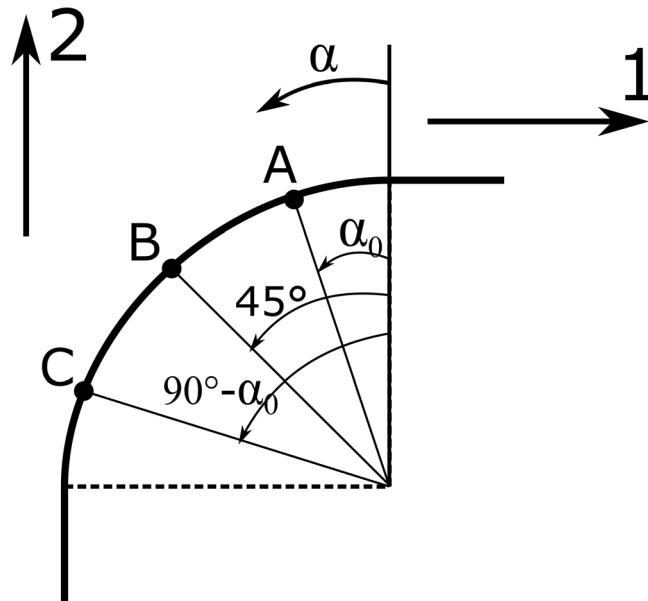


FIGURE 3 Points A, B and C are the locations where the components of the SCF matrix are calculated.

for all the load cases and geometries considered, despite the location of the maximum $\bar{\sigma}$ slightly fluctuates depending on the load ratios and the geometry. The position of A is calculated as to minimize the error between the equivalent stress concentration factor K_{eq} in the reference points and the actual maximum values, for all the geometries

considered and the load ratios R_1 , R_2 and R_{12} . The position of A is thus $\alpha_0 = 6^\circ$ and, consequently, C is located in $\alpha = 90^\circ - \alpha_0 = 84^\circ$.

1.2 | Fitting procedure

The FE simulations produced the values of each component of the SCF matrix as a function of the geometrical parameters for each of the critical A, B and C points. Analytical functions of the type of Equation (5) were subsequently obtained from these data by determining the coefficients via a fitting procedure, for each component and for each of the three points. The coefficients of Equation (5) are provided in the Supporting Information file in Section S1 for each location A, B and C.

$$K_{ij,ij} = A_1 + B_1 \left(\frac{R}{L}\right)^{C_1} + D_1 \left(\frac{t_0}{L}\right)^{E_1} + \frac{F_1}{Q_1 \left(\frac{R}{L}\right)^{G_1} + R_1 \left(\frac{t_0}{L}\right)^{H_1}} + I_1 \left(\frac{R}{L}\right)^{L_1} \left(\frac{t_0}{L}\right)^{M_1} + N_1 e^{(O_1 \left(\frac{R}{L}\right) + P_1 \left(\frac{t_0}{L}\right))} \quad (5)$$

Contour plots of K_{eq} for pure traction and pure shear and the total maximum relative error on K_{eq} between the model and the FE data as a function of t_0/L and R/L are shown in Figure S1, S2 and S3 in the Supporting Information (Section S2), respectively. The maximum error is below 10% in most of the domain, except in the case of sharp fillet radii and thick cell walls. In the use of such fitting model, the designer should be careful when working with $t_0/L > 0.15$ and $R/L < 0.02$. On the other hand, it must be considered that the maximum error is positive, meaning that the model overestimates the severity of the fillet. In other words, the model is conservative.

1.3 | Applicative example: Optimization tool

Probably the situation in which analytic functions can be the most useful are optimization problems. Let us consider a regular square cell lattice of finite size with filleted junctions loaded by a monoaxial distributed load (Figure 4a) and assume that we are interested in finding the geometrical parameters that minimize the stress concentration at the junctions while satisfying constraints on the elastic constants and on the geometrical parameters. Such problem could be encountered, for instance, in the design of fatigue resistant load bearing orthopaedic implants: the cellular lattice should have low stresses and an elastic modulus close to that of the human bone.¹² Let us also assume that the lattice principal directions 1–2 can have an inclination θ to the load direction, as shown in Figure 4a. The elastic constants of regular square cell lattices with filleted junctions of the same type discussed in this work can be easily calculated using semi-analytical functions developed by Dallago et al.⁹ The models assume plane stress behavior. The lattice is assumed to be made of a Ti alloy (elastic modulus $E_m = 110\text{GPa}$ and Poisson's ratio $\nu_m = 0.34$). The aim is to search the values of t_0/L , R/L and θ that minimize K_{eq} for a specific value E_0 of the elastic modulus in the load direction (E_{yy}). In this example, the geometrical parameters can assume any value inside the interval of validity of the semi-analytical model

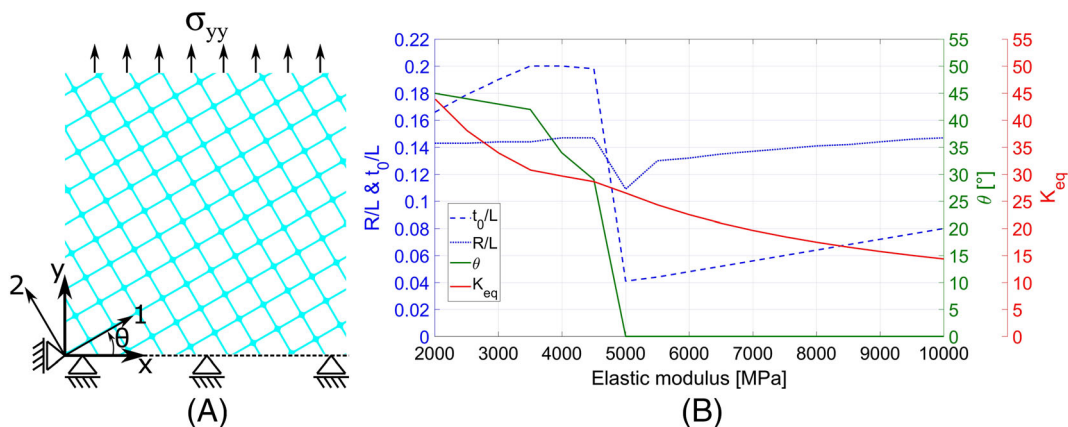


FIGURE 4 (a) Optimization problem: cellular lattice of finite size loaded by a monoaxial tension in direction y; (b) optimal geometrical parameters and K_{eq} as a function of the target stiffness of the structure in the loading direction.

TABLE 1 Comparison between the results of the optimization tool and FE simulations of a lattice of finite size. The error is defined as the difference between the model results and the FE results divided by the FE results.

Elastic modulus [MPa]	Optimal geometry			SCF from optimization	FE results		Error [%]	
	t_0/L	R/L	α [°]		K_{eq}	E_{yy} [MPa]	K_{eq}	E_{yy}
3000	0.19	0.144	43	33.9	33.9807	3013.4	0.19	0.34
4500	0.198	0.147	29	28.6	28.17837	4433.8	-1.55	-1.54
8000	0.064	0.141	0	17.4	17.6923	7946.2	1.45	-0.72

and because of the symmetry of the structure, the angle varies only between 0° and 45° . The multivariable optimization problem to solve becomes thus the following:

$$\begin{aligned} \text{Minimize:} \quad & K_{eq} = f\left(\frac{t_0}{L}, \frac{R}{L}, \sigma_1, \sigma_2, \tau_{12}\right) \\ \text{Subject to:} \quad & \left\{ \begin{array}{l} E_{yy} = f\left\{\frac{t_0}{L}, \frac{R}{L}, \alpha, E_m, \nu_m = E_0\right. \\ 0.02 \leq \frac{t_0}{L} \leq 0.2 \\ 0.01 \leq \frac{R}{L} \leq 0.15 \\ 0^\circ \leq \theta \leq 45^\circ \end{array} \right. \end{aligned}$$

The reader should note that further constraints can be included if appropriate, such as bounds on the relative density of the structure. The optimization problem was solved for several values of E_0 between 2 and 10 GPa and the results are shown in Figure 4b, where the optimal values of t_0/L , R/L and θ are plotted against the elastic modulus. In general, wide fillets and thick struts reduce the stress concentration at the junctions. Indeed, it is interesting to note that the fillet radius tends to be always the maximum allowed size, indicating a very strong influence of the fillet on the stresses. Therefore, to achieve low values of the elastic modulus but retain good fatigue resistance (as required, for instance, by biomedical lattices¹²) it is convenient to incline the material principal directions to the load so that bending actions are introduced into the lattice. On the other hand, if the requested elastic modulus is higher (as in other engineering applications, such as the automotive or the aeronautic sectors), aligning the load with the material principal directions seems the best solution to minimize the stresses.

The semi-analytical models used in this optimization procedures were developed considering one unit cell constrained by periodic boundary conditions. Consequently, they provide accurate solutions only if the unit cell is infinitesimally small compared to the lattice and there are no border effects: clearly, in engineering applications these conditions are never verified. Nevertheless, these models still provide reasonably accurate solutions for finite size lattices provided that the cells are small compared to the lattice dimension and far from the boundaries. Indeed, FE simulations were carried out to verify the results shown in Figure 4b for three values of the elastic modulus (3000, 4500 and 8000 MPa). A square lattice of side 10 times the unit cell length (which was fixed to 5 mm) with geometry determined by the optimal parameters corresponding to the appropriate elastic modulus was meshed with PLANE183 elements (plane stress behavior) and constrained as shown in Figure 4a. The stress field at a junction the furthest possible from the boundaries was estimated by transferring the displacement field to a submodel¹³ with a very fine mesh (Figure 2). The results of the semi-analytical model and the FE simulation are very close, with a deviation around 1% (Table 1).

2 | CONCLUSIONS

A model capable of calculating the SCFs at the cell wall junctions of 2D regular square cell lattices with filleted junctions was obtained by fitting parametric expressions to results of FE simulations. In such way a mathematical

relationship was found to define an equivalent stress concentration factor that appears to successfully relate the nominal homogenized loads in the cellular lattice to the local stress components at the filleted junctions. Compared to the results of FE simulations, the maximum error of such fitting model is below 10% for a wide range of the geometrical parameters. In the authors opinion, this work provides the designer with fast and useful design tools that avoid time-FE simulations. Indeed, a practical example demonstrates the potential of this approach in optimization problems. As future work, the authors aim to develop a similar model for the staggered lattices described by Dallago et al.⁹ and to improve the geometry of the junction by introducing variable radius fillets.¹⁴

CONFLICT OF INTEREST

The authors declare that they have no conflict of interest.

AUTHOR CONTRIBUTION STATEMENT

M. Dallago: simulations, literature review and manuscript draft.

S. Raghavendra, V. Fontanari and M. Benedetti: planning and revision.

ORCID

Michele Dallago  <https://orcid.org/0000-0002-3836-7583>

Matteo Benedetti  <https://orcid.org/0000-0001-9158-2429>

REFERENCES

1. Masoumi Khalil Abad E, Arabnejad Khanoki S, Pasini, D. Fatigue Design of Lattice Materials via Computational Mechanics: Application to Lattices with Smooth Transitions in Cell Geometry. *Int J Fatigue*. 2013;47:126-136. <https://doi.org/10.1016/j.ijfatigue.2012.08.003>
2. Huynh L, Rotella J, Sangid MD. Fatigue Behavior of IN718 Microtrusses Produced via Additive Manufacturing. *Mater Des*. 2016;105:278-289. <https://doi.org/10.1016/j.matdes.2016.05.032>
3. Dallago M, Winiarski B, Zanini F, Carmignato S, Benedetti M. On the Effect of Geometrical Imperfections and Defects on the Fatigue Strength of Cellular Lattice Structures Additively Manufactured via Selective Laser Melting. *Int J Fatigue*. 2019;124(March):348-360. <https://doi.org/10.1016/j.ijfatigue.2019.03.019>
4. Bagheri ZS, Melancon D, Liu L, Johnston RB, Pasini D. Compensation Strategy to Reduce Geometry and Mechanics Mismatches in Porous Biomaterials Built with Selective Laser Melting. *J Mech Behav Biomed Mater*. 2017;70:17-27. <https://doi.org/10.1016/j.jmbbm.2016.04.041>
5. Inglis CE. Stresses in a Plate Due to the Presence of Cracks and Sharp Corners. *Trans R Inst Nav Archit*. 1913;55:219-241.
6. Brock JS. Analytical Determination of the Stresses around Square Holes with Rounded Corners. *David Taylor Model Basin* 1957; No. Report 1149.
7. Sikora JP. A Summary of Stress Concentrations in the Vicinity of Openings in Ship Structures. *Nav. Sh. Res. Dev. Cent*. 1973; No. Report 3889.
8. Savin GN. *Stress Distribution Around Holes*. New York: Pergamon Press; 1961.
9. Dallago M, Benedetti M, Luchin V, Fontanari V. Orthotropic Elastic Constants of 2D Cellular Structures with Various Arranged Square Cells: The Effect of Filleted Wall Junctions. *Int J Mech Sci*. 2017; (122, December 2016):63-78. <https://doi.org/10.1016/j.ijmecsci.2016.12.026>
10. Bobyn JD, Tanzer M, Glassman AH. Stress-Related Bone Resorption. In: Shanbhag A, Rubash HE, Jacobs JJ, eds. *Joint Replacement and Bone Resorption: Pathology, Biomaterials, and Clinical Practice*. New York: Taylor & Francis; 2005.
11. Dowling NE. *Mechanical Behavior of Materials*. Fourth ed. London: Pearson Education; 2013.
12. Dallago M, Fontanari V, Torresani E, et al. Fatigue and Biological Properties of Ti-6Al-4 V ELI Cellular Structures with Various Arranged Cubic Cells Made by Selective Laser Melting. *J Mech Behav Biomed Mater*. 2018;78(October 2017):381-394. <https://doi.org/10.1016/j.jmbbm.2017.11.044>
13. ANSYS® Academic Research Mechanical, Release 18.1, Help System, Advanced Analysis Guide, ANSYS, Inc.
14. Berto F, Razavi J. Fatigueless Structures Inspired by Nature: A Case Study. *Mater Des Process Commun*. 2019; No. December 2018:1-3;1(3):e27. <https://doi.org/10.1002/mdp2.27>

SUPPORTING INFORMATION

Additional supporting information may be found online in the Supporting Information section at the end of the article.

How to cite this article: Dallago M, Raghavendra S, Fontanari V, Benedetti M. Stress concentration factors for planar square cell lattices with filleted junctions. *Mat Design Process Comm.* 2019;1–8. <https://doi.org/10.1002/mdp2.98>